Experimental studies of the influence of distributed power losses on the transparency of two-dimensional surface photonic band-gap structures

I. V. Konoplev,* A. D. R. Phelps, A. W. Cross, and K. Ronald
Department of Physics, University of Strathclyde, Glasgow, G4 0NG, United Kingdom
(Received 29 October 2002; revised manuscript received 11 July 2003; published 30 December 2003)

Two-dimensional (2D) surface photonic band-gap (SPBG) structures have been suggested to realize 2D distributed feedback. The 2D SPBG structures can be obtained by providing 2D periodic perturbations of the waveguide surface. Such a structure can be used in a wide variety of applications including microwave electronics and integrated optics. The theoretically predicted effect of the transparency of the 2D SPBG structure when distributed Ohmic losses inside the structure are relatively high in comparison with the wave coupling coefficient has been observed in a series of experiments. The results obtained are in good agreement with theoretical predictions.

DOI: 10.1103/PhysRevE.68.066613 PACS number(s): 42.70.−a, 84.40.−x, 42.79.Dj, 42.55.−f

I. INTRODUCTION

Two-dimensional (2D) Bragg structures have recently been under intensive theoretical [1–3] and experimental [4–6] study. These structures have been proposed for application in high-power microwave electronics [1] but can also be used in integrated optics [7,8]. It is well known and widely accepted that Bragg structures belong to the broad family of photonic band-gap (PBG) structures which are usually defined as periodic structures used to suppress the transmission of electromagnetic waves within a certain frequency range. The suppression of the transmission of the electromagnetic waves within a specific frequency range takes place mainly due to Bragg resonance scattering of the wave inside the PBG crystal. Let us note that there are many other common features between conventional PBG and Bragg structures used in microwave science and optics. These include both possessing a forbidden band gap located around the Bragg resonance frequency, and being distributed in nature with the suppression of the transmission dependence on a ''volume'' effect that exists due to resonant wave scattering on a periodic perturbation. Also the width of the forbidden band gap strongly depends on the ''contrast'' of the perturbation with respect to the unperturbed media, which in the case of Bragg structures corresponds to the amplitude of the corrugation. The main difference between the Bragg structures and conventional PBG crystals is that for a Bragg structure the periodicity is usually located on the wall of the guiding medium as opposed to a PBG, which is in the form of a periodic honeycomb volumelike material. It is therefore thought appropriate to differentiate the two by the use of the word ''surface.'' Further, we will refer to the Bragg structure studied as a surface photonic band-gap (SPBG) structure. This difference underlines the two limits of the application of the 2D model, where in a conventional 2D PBG crystal the length of perturbations is much larger than the operating wavelength (a conventional 2D PBG is often in the form of a structure made up of long rods), i.e., there is a very strong contrast between the perturbed and unperturbed media. In the Bragg structure studied in this paper the amplitude of the perturbations is small in comparison with the operating wavelength (periodic corrugations in the case presented), i.e., the system can be considered as a low ''contrast'' medium. This allows perturbation theory to be used, which leads to coupled-wave equations for specific modes propagating in the structure, while for the case of a strong contrast structure this approach will not work and the development of more complex theory in terms of Floquet-Bloch waves is required. Also, to the best of our knowledge, conventional PBG crystals are investigated in order to obtain a broad band gap for wave propagation resulting in unusual waveguide structures. In contrast, our goal is to obtain a narrowband highly selective, highly reflective mirror, which can also be used to obtain multidimensional distributed feedback and is a possible substitute for 1D Bragg structures which are used successfully in integrated optics and quantum oscillators.

The 2D SPBG structures studied in this paper can be obtained by providing 2D periodic corrugation of the waveguide surface or by lining the waveguide with a material that has a double periodicity of refractive index [8,9]. A schematic diagram of structures of coaxial geometry with periodic perturbation on the outer surface of the inner conductor is shown in Fig. 1. The black and white areas in the figure may either correspond to the recesses and untouched surface of the waveguide, or indicate the regions of high and low refractive index n of the lining material. It is important to note that similar 2D periodic planar structures have been considered (see, for example, [10–12]) to study the propagation of the slow surface waves (surface plasmon polaritons). Due to their nature the surface waves possess high Ohmic losses [11] but can be useful for signal processing in integrated optics and surface studies. Also, most of the energy of the surface wave is concentrated near the guiding surface (metal-dielectric interface) [12,13], which complicates the use of such waves for active high-power devices such as amplifiers and oscillators. In this work we study fast waveguide modes with relatively low Ohmic losses inside the waveguide and energy distributed between the waveguide's conductors. Such waves are attractive for application in op-

*Corresponding author. FAX: +44-141-552-2891. Email address: acp96115@strath.ac.uk

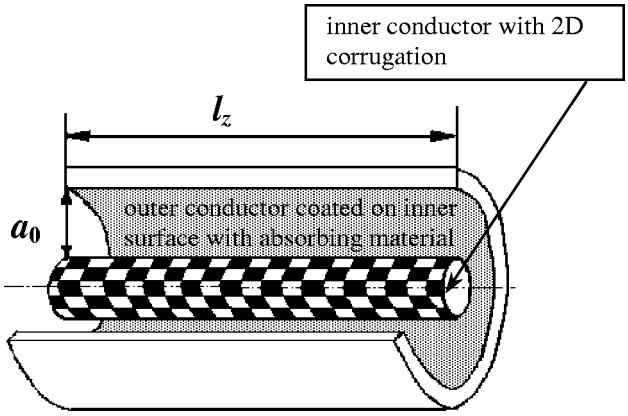

FIG. 1. Schematic diagram of 2D coaxial SPBG structure with corrugated inner and smooth outer conductors. The absorbing material painted on the inner surface of the outer conductor is indicated by gray shading.

tics communication, integrated optics, and use in high-power active devices.

The 2D periodic corrugation considered provides a 2D wave scattering such that counter propagating waves are coupled indirectly [Fig. 2(a)], unlike the 1D scattering. This allows the formation of a 2D feedback circle, which ensures mode selection over longitudinal and transverse wave indices as well as synchronization of radiation from the different parts of the oversized active medium. Computer simulations have shown that the additional fluxes of electromagnetic radiation result in synchronization of radiation from different parts of a grossly oversized [in the transverse dimension (up to 10^3 times of the operating wavelength)] active medium [1–3]. In recent studies [5,6] the existence of 2D scattering was demonstrated and operation of a free electron maser using a structure of planar geometry was reported [14].

The correlation between the wave absorption inside conventional PBG structures and wave transmission through such structures has recently been under investigation (see, for example, [15–18]). This issue is important because the losses inside the PBG structure may significantly affect the field evolution and therefore its performance. This paper is dedicated to an experimental study of the influence of the distributed power losses on the 2D SPBG structure transparency. In Sec. II a model and results obtained from a theoretical study of a structure with distributed power losses are discussed. In Sec. III the experimental setup and cold microwave measurements of such structures are presented. To conclude, we compare the experimental results with the theoretical predictions and discuss the possibility of using the phenomenon observed in high-power electronics and integrated optics.

II. MODEL AND THEORETICAL STUDY OF IDEAL COAXIAL 2D SPBG STRUCTURE

A coaxial ideal 2D structure consists of two conductors of radii $r_{\mathrm{in}}, r_{\mathrm{out}}$, length l_z, and having a small depth corrugation in the form

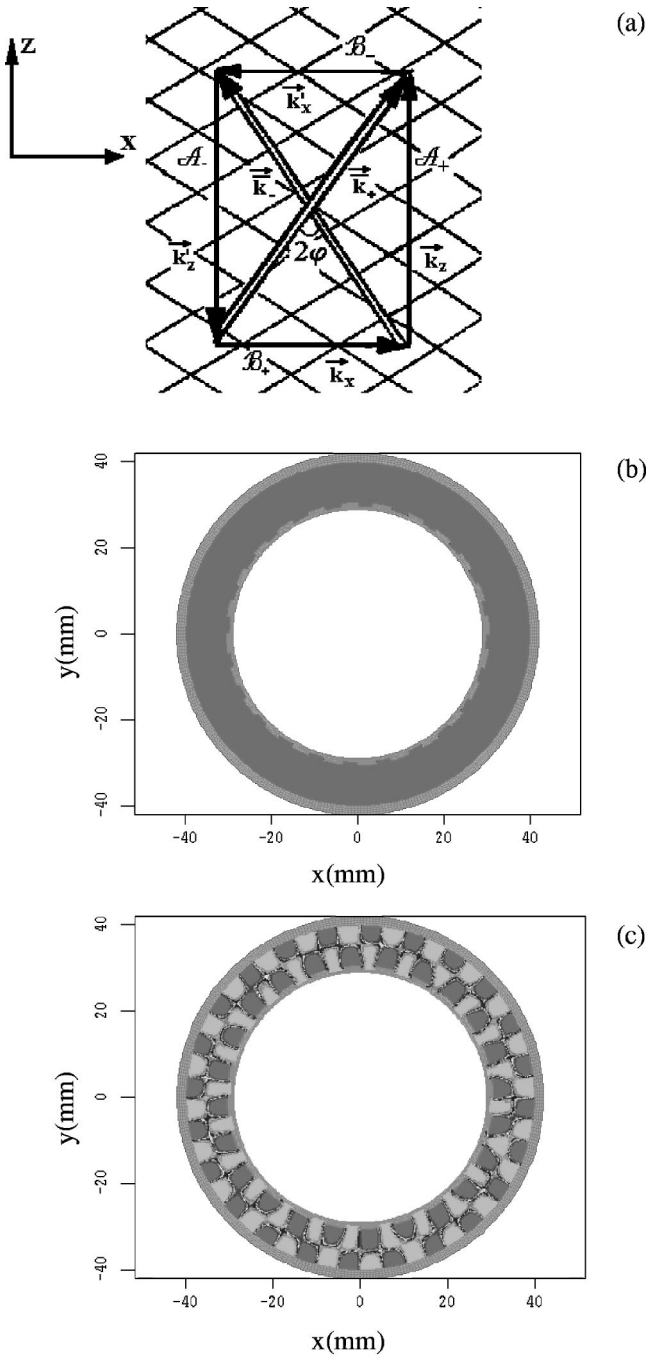

FIG. 2. (a) Schematic diagram of a two-dimensional distributed feedback loop realized on an ideal 2D corrugation. The snapshots of the profiles of the field components B_φ (b) and B_z (c) in the middle cross section of the 2D SPBG structure correspond to the magnetic field components of the partial waves $\mathcal{A}_\pm$ and $\mathcal{B}_\pm$, respectively.

$$a = a_1 \cos(\overline{k}_z z)\cos(\overline{m}\varphi), \tag{1}$$

where a_1 is the corrugation depth, $\overline{k}_z = 2\pi/d_z$, d_z is the period of the corrugation over the z coordinate, and $\overline{m}$ is the number of variations of the corrugation over the azimuthal coordinate [1–3]. We assume that the radii $r_{\mathrm{in}}, r_{\mathrm{out}}$ greatly exceed the distance between the conductors $a_0 = r_{\mathrm{out}} - r_{\mathrm{in}}$ and the radiation wavelength:

$$r_{\text{in,out}} \gg a_0, \quad r_{\text{in,out}} \gg \lambda. \tag{2}$$

Taking into account the conditions (2) the dispersion equation for the eigenwaves of the coaxial waveguide can be reduced to the following form [13]:

$$k^2 = \frac{\omega^2}{c^2} \cong k_z^2 + k_\perp^2, \tag{3}$$

where ω is the wave frequency, c is the speed of light, k_z is the longitudinal wave number, $k_\perp^2 = k_r^2 + k_\varphi^2$, $k_\varphi = M/r_0$ is the azimuthal wave number, $r_0 = (r_{\text{in}} + r_{\text{out}})/2$, $k_r = p\pi/a_0$ is the radial wave number, and M and p are the azimuthal and radial variation indices, respectively. The dispersion equation is similar to that obtained for the eigenwaves of the planar waveguide. This allows one to neglect the small curvature of the cavity surface and adopt the planar coordinate system, introducing the transverse coordinate $x = r_0 \times \varphi$, which enables k_x to be used instead of k_φ, i.e., $k_x \equiv k_\varphi$.

The field inside the 2D SPBG structure can be presented in the form of four coupled waves: $\mathcal{A}_\pm$, propagating in the $\pm z$ directions and $\mathcal{B}_\pm$, near cutoff waves "propagating" in the $\pm x$ directions (Fig. 2):

$$\vec{E} = \mathrm{Re}(\{\vec{E}_b^0(r)[\mathcal{B}_+(x,z)e^{-ik_x x} + \mathcal{B}_-(x,z)e^{ik_x' x}] + \vec{E}_a^0(r) \times [\mathcal{A}_+(x,z)e^{-ik_z z} + \mathcal{A}_-(x,z)e^{ik_z' z}]\}e^{i\omega t}). \tag{4}$$

Here $\mathcal{A}_\pm(x,z), \mathcal{B}_\pm(x,z)$ are slow functions of the x and z coordinates, k_x, k_x' and k_z, k_z' are the azimuthal and longitudinal wave numbers of the partial waves $\mathcal{B}_+, \mathcal{B}_-$ and $\mathcal{A}_+, \mathcal{A}_-$, respectively, and $E_{a,b}^0(r)$ are functions describing the spatial wave profile along the r coordinate, which coincides with one of the eigenmodes of the coaxial waveguide. We also assume that the distance between the inner and outer conductors is small to ensure the excitation of partial waves $\mathcal{B}_+$ and $\mathcal{B}_-$ with one specific radial wave number defined by the resonance conditions (see below). Due to the circular geometry of the coaxial system the wave amplitudes should satisfy the cyclic boundary conditions

$$\mathcal{B}_\pm(x + l_x, z) = \mathcal{B}_\pm(x,z), \quad \mathcal{A}_\pm(x + l_x, z) = \mathcal{A}_\pm(x,z), \tag{5}$$

where $l_x = 2\pi r_0$ is the cavity mean circumference. These conditions allow the partial wave amplitudes $\mathcal{A}_\pm(x,z), \mathcal{B}_\pm(x,z)$ to be represented in the Fourier series

$$\mathcal{A}_\pm(x,z) = \sum_{m=-\infty}^{\infty} \mathcal{A}_\pm^m(z) e^{imsx},$$

$$\mathcal{B}_\pm(x,z) = \sum_{m=-\infty}^{\infty} \mathcal{B}_\pm^m(z) e^{imsx}, \tag{6}$$

where $s = 2\pi/l_x$.

The lattice eigenvectors can be presented as $\vec{\bar{k}}_\pm = \bar{k}_x \vec{x}_0 \pm \bar{k}_z \vec{z}_0$, where $\vec{x}_0$ and $\vec{z}_0$ are the unit vectors along the x and z coordinates and $\bar{k}_x, \bar{k}_z$ are the amplitudes of the projections of the lattice eigenvectors $\vec{\bar{k}}_\pm$ on the axes x and z. In Fig. 2(a) the partial wave $\mathcal{A}_+$ propagating in the $+z$ direction is scattered into waves $\mathcal{B}_\pm$ propagating in the transverse $\pm x$ directions and scattering into waves $\mathcal{A}_\pm$, which ensures that the two-dimensional feedback loop $\mathcal{A}_+ \to \mathcal{B}_\pm \to \mathcal{A}_- \to \mathcal{B}_\pm \to \mathcal{A}_+$ is completed. To obtain an efficient coupling of the partial waves $\mathcal{A}_\pm \leftrightarrow \mathcal{B}_\pm$ the following Bragg resonance conditions [7,19] should be satisfied for each pair of coupled waves:

$$\vec{k}_z - \vec{k}_x = \vec{\bar{k}}_-, \quad \vec{k}_z' - \vec{k}_x' = -\vec{\bar{k}}_-, \tag{7a}$$

$$\vec{k}_z - \vec{k}_x' = \vec{\bar{k}}_+, \quad \vec{k}_z' - \vec{k}_x = -\vec{\bar{k}}_+. \tag{7b}$$

Taking into account that the 2D feedback loop can be obtained only when conditions (7) are satisfied simultaneously, the four partial waves undergo the coupling on the 2D structure if

$$k_z = k_z' \cong \bar{k}_z, \quad k_x = k_x' \cong \bar{k}_x \quad (|\bar{m}| = |M|) \quad \text{and} \quad |k_z| \simeq |k_\perp'|, \tag{8}$$

where $k_\perp'$ is the transverse wave number of the partial waves $\mathcal{B}_\pm$. The last condition in Eq. (8) does not follow from Eq. (7) but from the condition that the waves $\mathcal{B}_\pm$ should be near cutoff of the waveguide. In Fig. 2 the snapshots of the profiles of the incident (reflected) waves $\mathcal{A}_\pm$ ($\mathcal{A}_-$) [Fig. 2(b)] and waves $\mathcal{B}_\pm$ [Fig. 2(c)] are shown at the cross section, which corresponds to the center of the structure. These figures were obtained for the structure studied in the experiments using the 3D particle-in-cell (PIC) code MAGIC. The incident TEM wave has no field variation along the radial and azimuthal coordinate and the shading, which represents the polarity of the wave, does not change. The field component (B_z) observed in simulations and presented in Fig. 2(c) does not exist in the field of either incident or reflected TEM waves ($\mathcal{A}_\pm$) and can be attributed only to the near cutoff wave $\mathrm{TE}_{24,1}$ of the coaxial waveguide (partial waves $\mathcal{B}_\pm$). Thus the change of the polarity along the azimuthal and radial coordinates is obvious and 24 variations are clearly evident in Fig. 2(c). This agrees with the resonance conditions and the waveguide dispersion relation (8).

The field scattering on the corrugation, when conditions (8) are satisfied, can be described by the set of coupled wave equations for the dimensionless amplitudes $A_\pm, B_\pm$

$$\pm \frac{\partial A_\pm}{\partial z} + i\delta A_\pm + \sigma A_\pm + i\alpha(B_+ + B_-) = 0, \tag{9a}$$

$$\pm \frac{\partial B_\pm}{\partial x} + i\delta B_\pm + \sigma B_\pm + i\alpha(A_- + A_+) = 0, \tag{9b}$$

where $A_\pm = \mathcal{A}_\pm \hat{e}^{\mp i\delta z}$, $B_\pm = \mathcal{B}_\pm \hat{e}^{\mp i\delta x}$, $\delta = (\omega - \omega_0)/c$ is the small frequency detuning from the Bragg resonance, $\omega_0 = c\sqrt{\bar{k}^2 + k_r^2}$ is the Bragg frequency $|\omega - \omega_0| \ll \omega_0$, σ is the distributed power loss, and α is the wave coupling coefficient [1–3]. Substituting Eq. (6) in Eq. (9), the set of equations can be reduced to

$$\pm\frac{dA_{\pm}^{m}}{dz}+\frac{2\alpha^{2}(i\delta+\sigma)}{(i\delta+\sigma)^{2}+s^{2}m^{2}}(A_{+}^{m}+A_{-}^{m})+(i\delta+\sigma)A_{\pm}^{m}=0. \tag{10}$$

Let us note that the distributed power losses can be associated, for example, with Ohmic losses due to the skin effect or due to the presence of a dissipative material lining the surface of the waveguide.

The reflection and transmission coefficients from such a structure can be found by taking into account the following boundary conditions:

$$A_{+}^{m}(z=0)=A_{0}^{m}, \quad A_{-}^{m}(z=l_{z})=0, \tag{11}$$

where l_z is the length of the 2D structure. The analytic expressions for the reflection R_m and the transmission T_m coefficients can be obtained as functions of the azimuthal index m and frequency detuning δ_0 of the incident wave. Let us note that δ_0 is real, in contrast to δ which is complex:

$$R_{m}=\frac{\bar{\lambda}_{m}^{2}-p_{m}^{2}}{q_{m}[p_{m}-\bar{\lambda}_{m}\cot(\bar{\lambda}_{m}l_{z})]}, \tag{12}$$

$$T_{m}=\frac{-i\bar{\lambda}_{m}}{\sin(\bar{\lambda}_{m}l_{z})[p_{m}-i\bar{\lambda}_{m}\cot(\bar{\lambda}_{m}l_{z})]}, \tag{13}$$

where

$$q_{m}=\frac{2\alpha^{2}\tilde{\delta}}{s^{2}m^{2}+\tilde{\delta}^{2}}, \quad p_{m}=\frac{2\tilde{\delta}\alpha^{2}}{s^{2}m^{2}+\tilde{\delta}^{2}}+\tilde{\delta}, \quad \tilde{\delta}=i\delta_{0}+\sigma,$$

and

$$\bar{\lambda}_{m}=-i\tilde{\delta}\sqrt{\frac{4\alpha^{2}}{\tilde{\delta}^{2}+s^{2}m^{2}}+1}, \tag{14}$$

where σ is associated with the rf power losses. In analyzing expressions (12) and (13), we have to note that for each mode with index m such a structure provides an effective reflection zone (forbidden band gap), inside a frequency interval defined by the condition $\mathrm{Re}(\bar{\lambda}_{m}^{2})\leqslant 0$. In Fig. 3 the theoretical result obtained from the full 3D simulation of the experimental system using the PIG code MAGIC [Fig. 3(a)] and numerical analysis of Eq. (13), together with the experimental data obtained [Fig. 3(b)] are presented. The good agreement between the results presented is easy to see and proves the validity of the use of the coupled-wave approximation for the study of a low contrast structure.

It is important to note that in a real system the rf power losses are always present, while the coupling coefficient, which is proportional to the amplitude of the periodic perturbations, can be easily adjusted. Analyzing Eq. (10) together with conditions (11), the profiles of the partial waves, when the azimuthal-symmetric wave ($m=0$) is incident on the 2D structure at the exact Bragg frequency, are presented for three different values of α/σ. Thus when $\alpha/\sigma\gg 1$ [Fig. 4(a)]

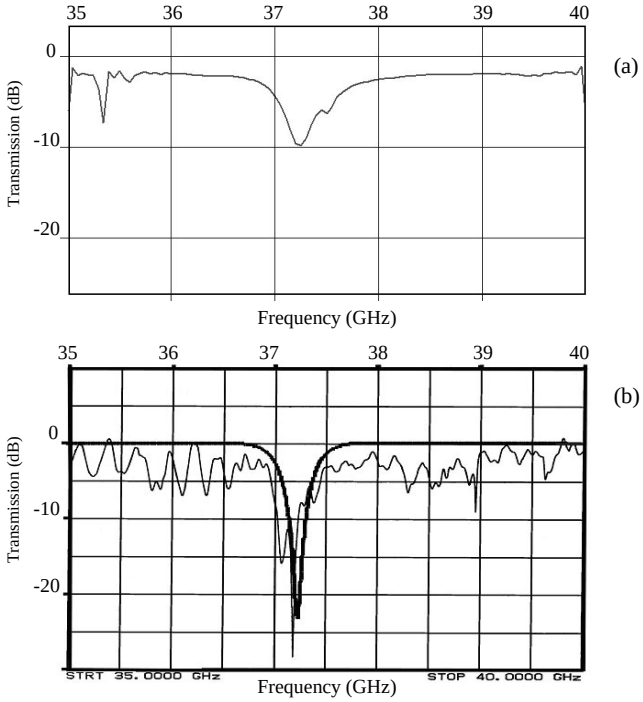

FIG. 3. The transmission coefficient through a 2D SPBG structure of length 4 cm obtained (a) from simulations using the 3D PIC code MAGIC and (b) from experimental results (thin line) and theoretical predictions using formula (13) (thick line).

the absolute values of the amplitudes of the waves $\mathcal{A}_{+}$ and $\mathcal{A}_{-}$ are nearly equal and $|R|\to 1$. Decrease of the parameter $\alpha/\sigma\sim 1$ [Fig. 4(b)] leads to a significant drop of the amplitude of the reflected $\mathcal{A}_{-}$ wave and an increase of the amplitude of the transmitted wave $\mathcal{A}_{+}(z=l_z)\sim 0.5$. When $\alpha/\sigma \ll 1$ [Fig. 4(c)] the amount of energy that passes from one partial wave into another due to scattering ($\alpha\neq 0$) is insufficient as compared to the energy dissipated, and the maximum reflection coefficient at the exact Bragg resonance frequency is of the order $\sim O(\alpha/\sigma)^2$. As a result the condition $\alpha\approx\sigma$ can be considered as the lower limit in the minimum value of the coupling coefficient, i.e., this dictates the minimum amplitude of the periodic perturbations. This also limits the minimum effective width of the reflection zone defined by $\mathrm{Re}(\bar{\lambda}_{m}^{2})\leqslant 0$. Let us note that if such a structure is used as mirror for an oscillator's cavity it is reasonable to assume that the parameter α/σ should be large for the input mirror and moderate for the output mirror in order to allow some radiation to escape out of the cavity. On the other hand the 2D SPBG structure can also be used in a high-power amplifier if α/σ is small. In this case the amplitude of the backward wave is insufficient to result in self-excitation of the system while at the same time transverse fluxes are still present, which are sufficient to synchronize the radiation from the different parts of the oversized medium.

Taking into account that in the experiments presented the 2D SPBG structures were excited with a TEM mode of a coaxial waveguide ($m=0$), the expression for the reflection coefficient (12) can be presented as

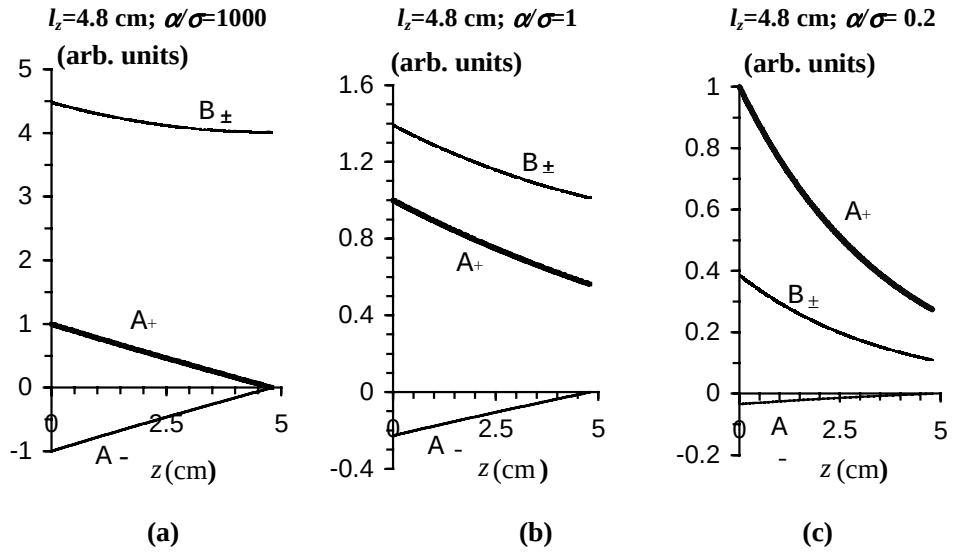

FIG. 4. Spatial profile of the partial waves $\mathcal{A}_{\pm}$ and $\mathcal{B}_{\pm}$. The partial wave $\mathcal{A}_{+}$ is the incident wave of unit amplitude (solid wide line) on the 2D SPBG structure: $l_z = 4.8$ cm, $s = 0.29\ \mathrm{cm}^{-1}$, and α/σ is (a) 1000; (b) 1; (c) 0.2

$$R_0 = \frac{-2\hat{\alpha}^2}{2\hat{\alpha}^2 - \delta^2 - i[\overline{\delta}(4\hat{\alpha}^2 - \delta^2)^{1/2}]\coth[l_z\sigma(4\hat{\alpha}^2 - \delta^2)^{1/2}]}, \tag{15}$$

where $\delta = (\delta_0/\sigma) - i$, $\hat{\alpha} = \alpha/\sigma$, $i = \sqrt{-1}$, and l_z is the length of the 2D SPBG structure. The dependence of the transmission coefficient for three different values of α/σ when $m = 0$ is presented in Fig. 5. The maxima of the reflection coefficients are located at exact Bragg frequencies [defined by Eq. (8)] and strongly depend on the parameter α/σ. In accordance with the previous discussion, when distributed losses are small in comparison with the value of the coupling coefficient, the minimum of the transmission is at the exact Bragg frequency and the effective width of the band gap is $\sim 4\alpha$. However, when $\alpha/\sigma \ll 1$ the amplitude of the drop of the transmission coefficient at exact Bragg resonance is $O(\alpha^2/\sigma^2)$ with respect to the transmission outside the band gap, and therefore the forbidden band gap may be relatively difficult to distinguish from the background noise, via measurement of the reflection/transmission coefficients. This effect of a ''disappearance'' of the sharp resonance drop of the transmission coefficient also exists for other modes with an index $m \neq 0$ [6]. From this point forward we will refer to this effect as a transparency of the 2D SPBG structure.

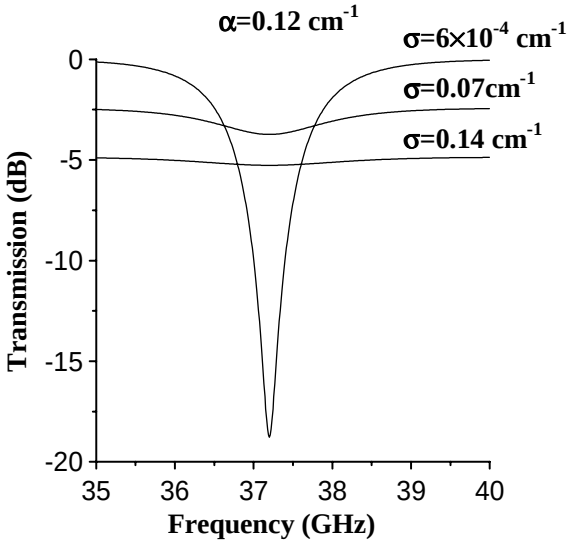

FIG. 5. Theoretically predicted frequency dependence of the power transmission through the 2D SPBG structure of length 4.8 cm and radii of inner and outer conductors 2.95 and 3.90 cm, respectively.

III. EXPERIMENTAL STUDY OF THE DISTRIBUTED POWER LOSS INFLUENCE ON THE 2D SPBG STRUCTURE TRANSPARENCY

The results of the experimental study of the influence of the distributed power losses on the 2D SPBG structure transparency are presented in this section. We aim to demonstrate the theoretically predicted transparency of the coaxial 2D SPBG structure when the ratio between distributed power losses σ and wave-coupling coefficient α is $\alpha/\sigma \leqslant 1$.

The 2D SPBG coaxial structure was obtained by providing a shallow 2D corrugation on the outer surface of the inner conductor of a coaxial waveguide (Fig. 1). It is important to note that the theoretical results were obtained for an ideal sinusoidal 2D corrugation (1), while in the experiments an ideal sinusoidal corrugation was substituted by a 2D ''square wave'' corrugation with a chessboard pattern [5,6] (Fig. 6). It was shown in [5,6] that this type of corrugation is a good substitution for the ideal sinusoidal corrugation. To obtain the required ''square wave'' corrugation, the inner conductor of the 2D SPBG structure (Fig. 6) was assembled from a set of separate gears. The length of each gear was a half period of the corrugation. To obtain the chessboard structure each gear was rotated with respect to the nearest gear at a specific angle, which is defined by the period of

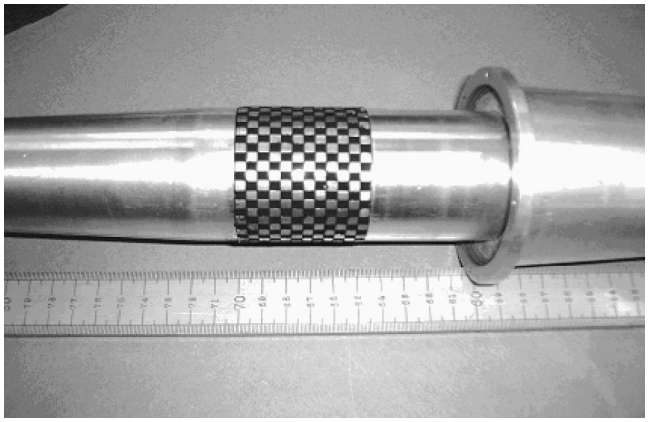

FIG. 6. Photograph of the 2D corrugated inner conductor of the 2D SPBG coaxial structure with chessboard corrugation pattern.

corrugation and the diameter of the inner conductor. This design allowed a simpler manufacturing technique to be used, which reduced the time required to construct such a structure. The geometry and parameters of the corrugation of the 2D SPBG coaxial structure coincided with those of a 2D SPBG structure [5] but of length 4.8 cm. To excite the 2D SPBG structures with a TEM mode of a coaxial waveguide, a special transmission line as described in previous experiments [5] was used. The microwave parameters of the structures were measured using a scalar network analyzer in the frequency range from 30 to 40 GHz. In accordance with the calculations, the minimum of the transmission was obtained at the resonance frequency 37.3 GHz, which corresponds to the cutoff frequency of the $TE_{24,1}$ wave of the coaxial waveguide. In the previous study [5] it was assumed that the partial waves $\mathcal{B}_{\pm}$ are $TM_{24,0}$ waves, but more detailed analysis (Fig. 2) demonstrated that the $TE_{24,1}$ mode is excited.

To conduct the experiments one has to vary the distributed losses while keeping the coupling coefficient constant. Changing the coupling coefficient while keeping the distributed power losses constant will result in broadening/narrowing of the band gap of the structure. Therefore, taking into account the strong noise interference, which is always present, the band narrowing may lead to unreliable results. Also, it is important to note that because the 2D SPBG structure was obtained by providing corrugation of the inner conductor of the coaxial waveguide and the coupling coefficient α is proportional to the ratio of the amplitude of the corrugation to the distance between the waveguide conductors, it was much easier to vary the distributed power losses rather than the wave-coupling coefficient. In the experiments the losses were gradually increased by increasing the number of layers of absorbing paint coated on the inner surface of the outer conductor. The maximum width of the absorbing material was less than 1 mm and much less than the distance between the inner and outer conductors. Before conducting the experiments with the 2D SPBG structures the losses were calibrated. To calibrate the rf power losses a smooth inner conductor was used. First, a ''clean'' outer conductor, i.e., an outer conductor without a coat of absorbing material was used. In this case the power losses inside the coaxial waveguide due to the skin effect can be estimated to be $\sigma = k\Delta(1/a + 1/b)/2\ln(a/b)$, where Δ is the skin depth for a specific material, a and b are the radii of the outer and inner conductors, and k is the wave number. Taking into account that $a = 3$ cm, $b = 4$ cm, $k \cong 7.81\ \mathrm{cm}^{-1}$, and the outer conductor was made from aluminum alloy, the loss parameter was estimated to be of value $\sigma \approx 6 \times 10^{-4}\ \mathrm{cm}^{-1}$. Transmission through part of the coaxial waveguide, when medium- [Fig. 7(a), bold line] and high-power [Fig. 7(b), bold line] losses were introduced, were compared with the power transmitted through the coaxial waveguide when no absorbing material was present [Figs. 7(a) and 7(b), thin line]. In the frequency region of the expected band gap (37–38 GHz) the attenuation was approximately 2.5 dB ($\approx$0.6 dB/cm or $\sigma \approx 0.07\ \mathrm{cm}^{-1}$) for the medium-loss absorbing coating and approximately 5 dB ($\approx$1.25 dB/cm or $\sigma \approx 0.14\ \mathrm{cm}^{-1}$) for a high-loss absorbing coating.

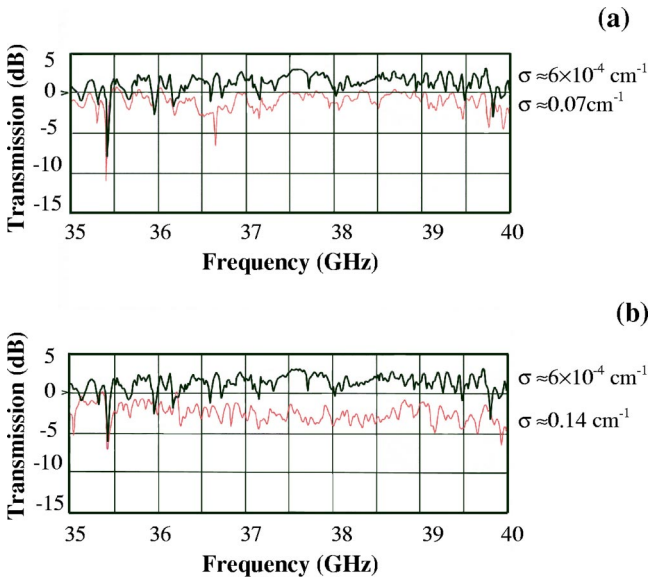

FIG. 7. Frequency dependence of the power transmission through part of a coaxial waveguide of length 4.8 cm, radii of inner and outer conductors 2.95 and 3.90 cm, respectively, with (a) unmodified (bold line) and added medium (thin line) losses; (b) unmodified (bold line) and added high (thin line) losses.

After the calibration of the rf power losses, the smooth inner conductor was substituted with the corrugated one. Taking into account the parameters of the structure the coupling coefficient was estimated to be $\alpha \approx 0.12\ \mathrm{cm}^{-1}$. The results of the computer simulations of the power transmitted through the 2D SPBG structures with the wave-coupling coefficient $\alpha \approx 0.12\ \mathrm{cm}^{-1}$ and different values of distributed losses are presented in Fig. 5. The experimental results of measurement of transmission coefficients through the 2D SPBG structure are presented in Figs. 8 and 9. Comparing Figs. 8 and 5, one notes that when low-absorption material was used ($\alpha/\sigma \gg 1$) the forbidden band gap is clearly evident in both figures. In Figs. 8(a) and 8(b) the thin line indicates the transmission through the 2D SPBG structure with low losses. When a medium-loss absorbing material was used, $\alpha/\sigma \geqslant 1$, Fig. 8(a) (bold line), the shape and amplitude of the transmission forbidden gap were significantly changed (compare with Fig. 5). Further increase of $\alpha/\sigma \leqslant 1$, Fig. 8(b) (bold

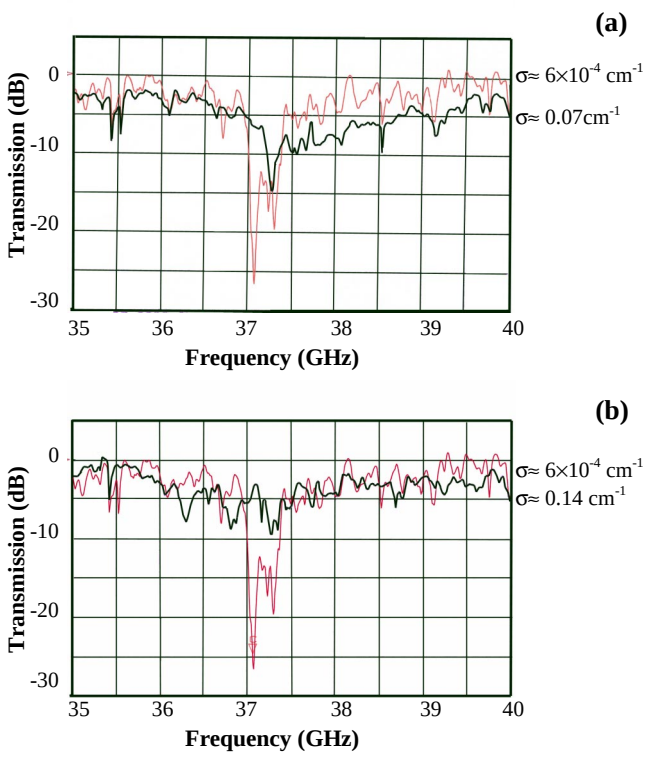

FIG. 8. Comparison of the frequency dependence of the power transmission through the 2D SPBG structure without added losses (thin line) with the frequency dependence of the power transmission (bold line) when added losses are (a) medium and (b) high.

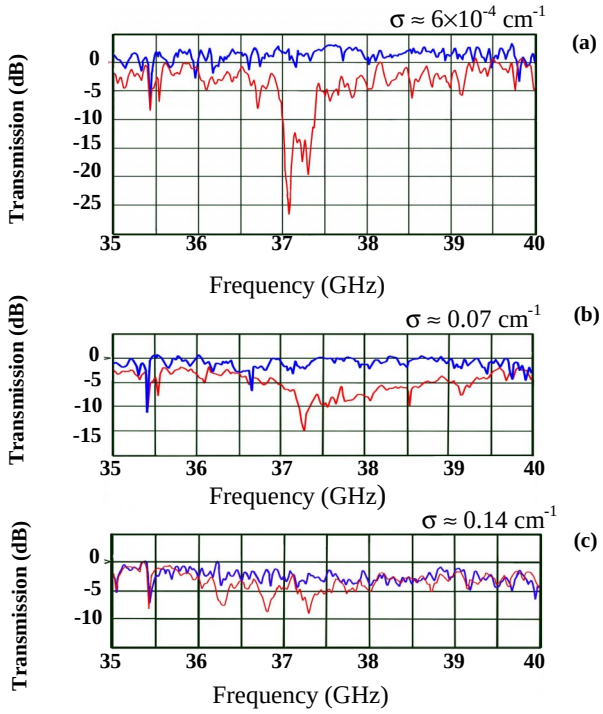

FIG. 9. Frequency dependence of the power transmission through the part of coaxial waveguide (bold line) and 2D SPBG structure (thin line) of length 4.8 cm when there are (a) no added losses; (b) added medium losses; (c) added high losses.

line) resulted in a ''disappearance'' of the transmission forbidden gap. In Fig. 9 a comparison of the transmission through coaxial structures with a corrugated (thin line) and a smooth (bold line) inner conductor are presented. The 2D SPBG structure's forbidden band gap is clearly visible when Ohmic losses are low [Fig. 9(a)] and are less visible when medium-level losses are introduced [Fig. 9(b)]. The difference between transmission coefficients through the structure with the smooth and the corrugated inner conductors becomes negligible when high Ohmic losses are introduced [Fig. 9(c)]. In this case, the 2D SPBG structure can be considered as ''transparent'' as a part of the coaxial line but with added power losses. Comparing Fig. 5 with Figs. 8 and 9 it is clear that the experimental data agreed rather well with the theoretical predictions.

IV. CONCLUSION

An experimental study of the influence of rf power distributed losses on the 2D SPBG structure transmission coefficient has been carried out. Measurement of the transmission coefficient was conducted for different values of distributed losses while all other parameters of the 2D SPBG structure were held constant. Observation of the transparency of the 2D SPBG structure was completed and comparison of the data obtained from experiments with theoretical analysis demonstrated that the experimental results agreed well with theoretical predictions. It is important to note that in the frequency regions far from resonance the transmission features are reproducible in all the experiments that were conducted. Let us also note that a similar correlation between wave absorption and transmission has been obtained for conventional PBG structures [15–18]; however, it was observed only at the edges of the band gap. In contrast with our results, which demonstrate that the band gap ''disappears'' due to an increase of the wave absorption, the increased absorption in [15–17] was explained by increased transparency of the structures at those band-gap edge frequencies and therefore increased probability for the light to be absorbed. The results do not contradict each other but underline two different effects obtained in [15–18] and in the work presented in this paper. This also follows from previous studies [20–22] in which a similar effect for conventional 2D PBG and 3D PBG structures has been obtained. Thus in Ref. [20] it was shown that in conventional 2D PBG structures the band gap appears only when the dielectric contrast ratio is 7.2, and if the contrast is reduced this leads to ''disappearance'' of the band gap. This was also obtained for the 3D PBG structure [22] where changing the contrast ratio from 12 to 4 resulted in a decrease of the photonic band-gap width, while further reduction of the ratio has resulted in a complete ''disappearance'' of the band gap. Let us note that the wave-coupling coefficient is proportional to the medium's contrast.

By extending the concept of the experiments presented in the paper, it becomes rather obvious that if the resistivity of the absorbing material or coupling coefficient is sensitive to external influence such as temperature, magnetic field, or laser radiation then induced transparency may be observed.

This can be used to obtain fast optical switches, active mirrors, and filters. Thus the use of a 2D biperiodic dielectric instead of a biperiodic corrugation can be considered. Using the results obtained above, it is easy to foresee that, if a nonlinear medium with a double periodic refractive index (see, for example, [9]) is used, i.e., when the perturbed refractive index of the medium n_1 is dependent on the field intensity and n_0 is the refractive index of the unperturbed medium, a nonlinear change of the width of the band gap due to a change of the coupling coefficient (ratio n_1/n_0), as well as induced transparency, may be observed. The theory and experiments also predict that a band gap will appear only when the coupling coefficient, i.e., the ratio n_1/n_0 is larger than some threshold value, which is defined by distributed losses inside the structure, which can be due to either Ohmic losses in the medium, or diffraction losses. The set of equations describing the field evolution inside the structure should now be presented in a time-dependent form [3] with a modified coupling coefficient:

$$\frac{\partial A_+}{\partial Z}+\frac{\partial A_+}{\partial \tau}+\sigma(I,F)A_+ + i\hat{\alpha}(I,F)(B_+ + B_-)=0,$$

$$-\frac{\partial A_-}{\partial Z}+\frac{\partial A_-}{\partial \tau}-\sigma(I,F)A_- + i\hat{\alpha}(I,F)(B_+ + B_-)=0,$$

$$\pm\frac{\partial B_\pm}{\partial X}+\frac{\partial B_\pm}{\partial \tau}+\sigma(I,F)B_\pm + i\hat{\alpha}(I,F)(A_+ + A_-)=0, \tag{16}$$

where $\sigma(I,F)$ and $\hat{\alpha}(I,F)$ are some functions of field intensity $I=|\vec{E}|^2$ and the external parameter F, which can also influence the losses and the wave coupling.

ACKNOWLEDGMENTS

The authors would like to thank Professor G. G. Denisov for his help with the design of the mode converters and Professor N. S. Ginzburg, Dr. N. Yu. Peskov, and Dr. A. S. Sergeev for useful discussions. The authors would like to thank the EPSRC and QinetiQ for partial support of this work.

[1] N. S. Ginzburg, N. Yu. Peskov, and A. S. Sergeev, Opt. Commun. **112**, 151 (1994).
[2] N. S. Ginzburg, N. Yu. Peskov, A. S. Sergeev, A. D. R. Phelps, I. V. Konoplev, G. R. M. Robb, A. W. Cross, A. V. Arzhannikov, and S. L. Sinitsky, Phys. Rev. E **60**, 935 (1999).
[3] N. S. Ginzburg, N. Yu. Peskov, A. S. Sergeev, I. V. Konoplev, A. W. Cross, A. D. R. Phelps, G. R. M. Robb, K. Ronald, W. He, and C. G. Whyte, J. Appl. Phys. **92**, 1619 (2002).
[4] N. V. Agarin, A. V. Arzhannikov, V. B. Bobylev, N. S. Ginzburg, V. G. Ivanenko, P. V. Kalinin, S. A. Kuznetsov, N. Yu. Peskov, A. S. Sergeev, S. L. Sinitsky, and V. D. Stepanov, Nucl. Instrum. Methods Phys. Res. A **445**, 222 (2000).
[5] A. W. Cross, I. V. Konoplev, K. Ronald, A. D. R. Phelps, W. He, C. G. Whyte, N. S. Ginzburg, N. Yu. Peskov, and A. S. Sergeev, Appl. Phys. Lett. **80**, 1517 (2002).
[6] A. W. Cross, W. He, I. V. Konoplev, A. D. R. Phelps, K. Ronald, G. R. M. Robb, C. G. Whyte, N. S. Ginzburg, N. Yu. Peskov, and A. S. Sergeev, Nucl. Instrum. Methods Phys. Res. A **475**, 164 (2001).
[7] A Yariv, *Optical Electronics*, 3rd ed. (Holt-Saunders, Tokyo, Japan, 1985).
[8] N. Akozbek and S. John, Phys. Rev. E **57**, 2287 (1998).
[9] A. K. Sarychev and V. M. Shalaev, Phys. Rep. **35**, 275 (2000).
[10] S. I. Bozhevolnyi and F. A. Pudonin, Phys. Rev. Lett. **78**, 2823 (1997).
[11] S. I. Bozhevolnyi, J. Erland, K. Leosson, P. M. W. Skovgaard, and J. M. Hvam, Phys. Rev. Lett. **86**, 3008 (2001).
[12] S. C. Kitson, W. L. Barnes, and J. R. Sambles, Phys. Rev. Lett. **77**, 2670 (1996).
[13] L. A. Weinstein (Vainstein), *Electromagnetic Waves*, 2nd ed. (Radio i Sviaz, Moscow, 1988).
[14] N. S. Ginzburg, N. Yu. Peskov, A. S. Sergeev, A. V. Arzhannikov, S. L. Sinitsky, P. V. Kalinin, A. D. R. Phelps, and A. W. Cross, Nucl. Instrum. Methods Phys. Res. A **475**, 287 (2001).
[15] M. M. Sigalas, C. T. Chan, K. M. Ho, and C. M. Soukoulis, Phys. Rev. B **52**, 11744 (1995).
[16] Lie-Ming Li and Zhao-Qing Zhang, Phys. Rev. B **58**, 9587 (1998).
[17] V. Yannopapas, A. Modinos, and N. Stefanou, Phys. Rev. B **60**, 5359 (1999).
[18] A. Moroz, Phys. Rev. B **66**, 115109 (2002).
[19] N. F. Kovalev, I. M. Orlova, and M. I. Petelin, Izv. Vyssh. Uchebn. Zaved., Radiofiz. **11**, 783 (1967) (in Russian).
[20] E. Yablonovitch and T. J. Gmitter, Phys. Rev. Lett. **63**, 1950 (1989).
[21] R. D. Meade, K. D. Brommer, A. M. Rappe, and J. D. Joannopoulos, Appl. Phys. Lett. **61**, 495 (1992).
[22] S. G. Johnson and J. D. Joannopoulos, Appl. Phys. Lett. **77**, 3490 (2000).